Remote estimation of terrestrial evapotranspiration without using meteorological data

Yuting Yang,[1] Di Long,[2] and Songhao Shang[1]

Received 28 February 2013; revised 4 April 2013; accepted 5 April 2013; published 17 June 2013.

[1] We developed a new method to estimate terrestrial evapotranspiration (ET) from satellite data without using meteorological inputs. By analyzing observations from 20 eddy covariance tower sites across continental North America, we found a strong relationship between monthly gross primary production (GPP) and ET ($R^2 = 0.72$–0.97), implying the potential of using the remotely sensed GPP to invert ET. We therefore adopted the Temperature-Greenness model which calculates 16 day GPP using MODIS EVI and LST products to estimate GPP and then to calculate ET by dividing GPP with ecosystem water use efficiency (the ratio of GPP to ET). The proposed method estimated 16 day ET very well by comparison with tower-based measurements ($R^2 = 0.84$, $p < 0.001$, $n = 1290$) and provided better ET estimates than the MODIS ET product. This suggests that routine estimation of ET from satellite remote sensing without using fine-resolution meteorological fields is possible and can be very useful for studying water and carbon cycles. **Citation:** Yang, Y., D. Long, and S. Shang (2013), Remote estimation of terrestrial evapotranspiration without using meteorological data, *Geophys. Res. Lett.*, *40*, 3026–3030, doi:10.1002/grl.50450.

1. Introduction

[2] Land surface evapotranspiration (ET) is a key component of the water and energy balance over terrestrial ecosystems [*Oki and Kanae*, 2006]. Among many methods of ET quantification, satellite remote sensing has been shown to be one of the most promising ways of mapping ET over larger areas [e.g., *Bastiaanssen et al*., 1998; *Norman et al*., 1995]. Numerous models with varying structure and complexities have been developed to derive ET from remotely sensed variables (e.g., land surface temperature, LST, and vegetation index, VI) in combination with concurrent meteorological measurements (e.g., near surface air temperature and vapor pressure) [e.g., *Bastiaanssen et al*., 1998; *Long and Singh*, 2012; *Lu and Zhuang*, 2010; *Norman et al*., 1995; *Su*, 2002; *Yang and Shang*, 2013]. With increasing spatial and temporal resolutions of satellite images, meteorological inputs at sufficient temporal and spatial scales corresponding to those of satellite images are required but infrequently available. For example, the Moderate Resolution Imaging Spectroradiometer (MODIS) Global Terrestrial Evapotranspiration Product (MOD16) adopts Global Modeling and Assimilation Office meteorological data at 1° latitude 1.25° longitude resolution and uses the version 4 0.05° Climate Modeling Grid albedo as a major model input [*Mu et al*., 2011]. This is much too coarse with respect to 1 km 1 km MODIS pixel, and the mismatch in spatial resolution among the three input data sets is a key limitation of MOD16, especially for regions with strong climatic gradients.

[3] Although it would be possible to improve the spatial resolution of meteorological fields, it is worthwhile exploring methods to estimate ET only from remotely sensed information. This would substantially reduce the input effort and therefore increase the robustness of satellite-based ET models. The idea lies in use of some variables which are highly correlated with ET and have the potential to be estimated based entirely on remote sensing.

[4] ET consists of two components, evaporation (E) from the soil and transpiration (T) from the vegetation canopy. Because photosynthesis and transpiration are both biologically regulated by plant stomata and T generally dominates ET over vegetated surfaces, gross primary production (GPP) is considered valuable to infer ET over large areas only using satellite data [*Beer et al*., 2009; *Zhang et al*., 2009]. Existing studies have shown that use of remote sensing data solely can provide reasonable GPP estimates across a wide range of vegetation types [*Rahman et al*., 2005; *Sims et al*., 2008; *Peng et al*., 2013]. Moreover, the ratio of GPP to ET, known as the ecosystem water use efficiency (WUE), was found to be fairly constant over time for certain ecosystems [*Beer et al*., 2007; *Beer et al*., 2009; *Law et al*., 2002]. Therefore, once the among-site variability of WUE is well assessed, ET can be estimated from remotely sensed GPP. The objective of this study is to develop a method to estimate ET using remotely sensed GPP. ET estimates from the developed method were evaluated with eddy covariance measurements within the Ameriflux network.

2. Site, Data, and Methods

2.1. Flux Site Data

[5] Data from 20 sites within the Ameriflux network (http://public.ornl.gov/ameriflux) were used to develop and evaluate the new method (Table 1 and also see auxiliary material). These sites represent a wide diversity of bioclimate across North America. For each site, daily values of GPP and ET accumulated from half-hourly measurements of net ecosystem exchange and latent heat by eddy covariance

Additional supporting information may be found in the online version of this article.

[1]State Key Laboratory of Hydroscience and Engineering, Tsinghua University, Beijing, China.
[2]Bureau of Economic Geology, Jackson School of Geosciences, The University of Texas at Austin, Austin, Texas, USA.

Corresponding author: Y. Yang, State Key Laboratory of Hydroscience and Engineering, Tsinghua University, Beijing 100084, China. (yyt08@mails.tsinghua.edu.cn)

0094-8276/13/10.1002/grl.50450

Table 1. Descriptions of the Flux Sites in This Study, Including Site Identifier (Site ID), Plant Functional Type (PFT), Latitude (Lat, °N), Longitude (Lon,°°W), Data Period, Observed Water Use Efficiency (WUE) , Coefficient of Determination Between Observed Monthly GPP and Monthly ET (R^2), and Reference

Site ID	PFTa	Lat	Lon	Data period	WUE	R^2	Reference
US_Ha1	DBF	42.54	−72.17	2001–2005	3.40	0.97	*Urbanski et al.* [2007]
US_WCr	DBF	45.81	−90.08	2001–2006	3.67	0.93	*Cook et al*., 2008
US_MMS	DBF	39.32	−86.41	2001–2006	2.31	0.90	*Dragoni et al.* [2007]
US_Bar	DBF	44.07	−71.29	2004–2006	3.66	0.89	*Jenkins et al.* [2007]
US_MOz	DBF	38.74	−92.20	2004–2007	2.29	0.95	*Gu et al.* [2007]
US_Me2	ENF	44.45	−121.55	2002, 2004–2007	3.14	0.80	*Irvine et al.* [2007]
CA_NS1	ENF	55.88	−98.48	2002–2005	2.12	0.87	*Goulden et al.* [2006]
CA_NS2	ENF	55.91	−98.53	2002–2005	1.91	0.93	*Goulden et al.* [2006]
CA_NS3	ENF	55.91	−98.38	2001–2005	2.19	0.87	*Goulden et al.* [2006]
CA_NS4	ENF	55.91	−98.38	2002–2004	2.00	0.86	*Goulden et al.* [2006]
CA_NS5	ENF	55.86	−98.49	2001–2005	2.93	0.94	*Goulden et al.* [2006]
US_Wrc	ENF	45.82	−129.95	2001–2006	3.21	0.72	*Paw et al.* [2004]
US_Syv	MF	46.24	−89.35	2001–2005	3.39	0.95	*Desai et al.* [2005]
US_LPH	MF	42.54	−72.19	2002–2005	2.77	0.95	*Hadley et al.* [2008]
US_Ho1	MF	45.20	−68.74	2001–2004	4.27	0.93	*Hollinger et al.* [2004]
US_NC1	MF	35.81	−76.71	2005–2006	1.73	0.93	*Noormets et al.* [2010]
US_Fuf	Savanna	35.09	−111.76	2005–2007	1.69	0.86	*Dore et al.* [2008]
CA_NS6	Shrub	55.92	−98.96	2001–2005	1.47	0.85	*Goulden et al.* [2006]
CA_NS7	Shrub	56.64	−99.95	2005–2005	1.14	0.84	*Goulden et al.* [2006]
US_Var	Grass	38.41	−120.95	2001–2007	2.4	0.88	*Ma et al.* [2007]

systems were used. Data quantity control was described in publications listed in Table 1. Daily data were further summed up to obtain monthly GPP and ET values. Months with data gap longer than 3 days were discarded from this analysis. In addition to flux data, biological and ancillary data, such as leaf area index and soil texture, were also acquired.

2.2. Remote Sensing Data

[6] To estimate GPP, two MODIS land surface products were used in this study (from the Oak Ridge National Laboratory's Distributed Active Archive Center, http://www.modis.ornl.gov/modis/), including Enhanced Vegetation Index (EVI) and LST. EVI was obtained from the 16 day Terra MODIS vegetation index product (MOD13Q1, 250 m), and LST was acquired from the 8 day LST and Emissivity product (MOD11A2, 1000 m). The LST data were averaged with two consecutive periods of the data in order to conform to the 16 day MODIS EVI data. Only EVI data with aerosol values listed as "low" and the "usefulness" values greater than 8 (on a scale of 0–10) and LST data marked as cloud free were used. Following *Sims et al.* [2006], all data were extracted from 3 km × 3 km area centered on the flux tower.

2.3. Ecosystem Water Use Efficiency

[7] The coefficient of determination (R^2) between monthly GPP and ET for the 20 sites ranges from 0.72 to 0.97 (Table 1 and also see auxiliary material), demonstrating that WUE of the ecosystem remains generally invariant at the monthly scale. Then, WUE for each site was calculated from

$$\mathrm{WUE} = \sum_n \mathrm{GPP}\left(\sum_n \mathrm{ET}\right)^{-1} \tag{1}$$

where n is the number of months with available data.

[8] Ecosystem WUE varies by a factor of ~3 among sites (Figure 1), which is mainly attributed to environmental gradients. Following *Beer et al.* [2009], we regressed WUE to two stable environment properties ($R^2 = 0.82$, $p < 0.001$, $n = 20$),

$$\mathrm{WUE} = a_1\theta_F + a_2\left(1\text{-}e^{k_c \mathrm{LAI}_{\max}}\right) \tag{2}$$

where a_1 and a_2 are regression coefficients (see auxiliary material), θ_F is volumetric soil water content at field capacity, and $\mathrm{LAI}_{\max}$ is the maximum leaf area index during the data period. In this study, θ_F was estimated to be the water content retained in the soil at −0.02 MPa of suction pressure, which is midway of most reported θ_F values (−0.01 to −0.033 MPa) [*Haise et al.*, 1954; *Lei et al.*, 1988]. The VG-M model [*Van Genuchten*, 1980] was adopted to describe the soil water retention curve, and the parameters of the VG-M model for each site were estimated from measured soil texture and bulk density using the method given by *Schaap et al* [1998]. The exponential function of $\mathrm{LAI}_{\max}$ in equation (2) corresponds to the fraction of absorbed sunlight in the photosynthetic active radiation (PAR) domain. k_c is the extinction coefficient of radiation attenuation and is set to be 0.6.

[9] The leave-one-out cross validation is performed to test equation (2) (Figure 1). The estimated WUE agrees fairly well with observed ones ($R^2 = 0.80$, $p < 0.001$, $n = 20$; see auxiliary material). These estimated WUE values were later used to invert ET in combination with remotely sensed GPP.

2.4. ET Estimation

[10] Since ecosystem WUE remains fairly invariant at the monthly scale, monthly ET can be calculated by dividing monthly GPP with WUE (i.e., ET = GPP/WUE). However, to be consistent with the temporal scale of the MODIS data, we calculated ET at a 16 day interval here by assuming that the 16 day WUE is also relatively constant. It is assumed that short-term (e.g., days and subdays) fluctuations in WUE can be effectively eliminated at the 16 day time scale.

[11] We chose the Temperature-Greenness (TG) model proposed by *Sims et al.* [2008] to estimate 16 day GPP. It was successfully applied to estimate 16 day GPP for evergreen and deciduous forests in North America [*Sims et al.*,

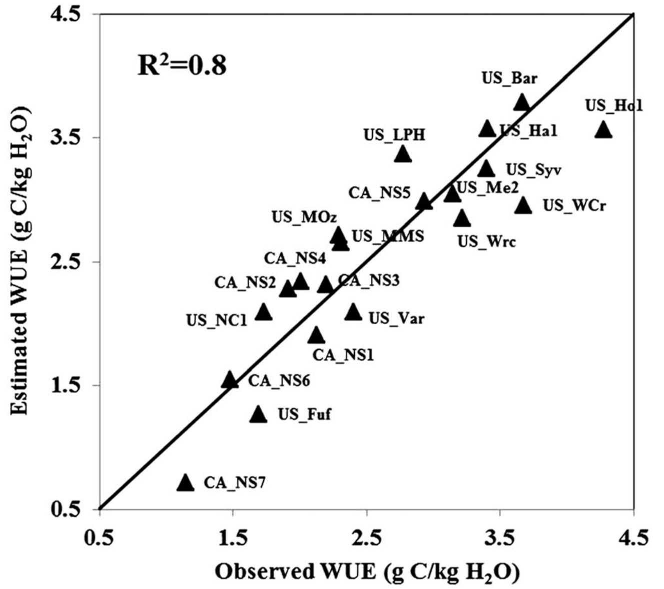

Figure 1. Validation of bivariate regression WUE $=f(\theta_F$, LAI$_{max})$ by leaving one out each time. Coefficient of determination between estimated and observed WUE; 1:1 line and site ID are shown.

2008]. The TG model estimates GPP using a combination of MODIS LST and EVI products at the 16 day interval as

$$\mathrm{GPP} = m\_\mathrm{TG} \times \mathrm{R\_EVI} \times \mathrm{R\_LST} \tag{3}$$

$$\mathrm{R\_EVI} = \mathrm{EVI} - 0.1 \tag{4}$$

$$\mathrm{R\_LST} = \min\left[\left(\frac{\mathrm{LST}}{30}\right), (2.5 - 0.05 \times \mathrm{LST})\right] \tag{5}$$

where *m*_TG is the coefficient which can be estimated as a function of annual mean nighttime LST [Sims et al., 2008]. Equation (4) indicates a zero GPP when EVI is smaller than 0.1, and equation (5) indicates that the value of R_LST changes linearly between 1 when LST is 30°C and 0 when LST is 0 °C or 50 °C.

3. Results and Discussion

[12] Overall, the proposed approach estimated 16 day ET reasonably well with reference to tower-based measurements ($R^2 = 0.84$, $p < 0.001$, $n = 1290$). The root-mean-square error (RMSE) ranges from 0.16 to 0.72 mm/d and the mean relative error (MRE) are found between 0.6% and 38.6% (Table 1). The bias in ET estimation results mostly from errors in modeled WUE from equation (2). For example, at US_WCr, equation (2) underestimates WUE by 19.3%, which results in a 15.8% overestimation of ET. The residual bias may be explained by error in *m*_TG estimates.

[13] Larger scatters of the relationship between observed and estimated ET are found at the US_Me2 ($R^2 = 0.64$, $p = 0.001$, $n = 57$) and US_Fuf sites ($R^2 = 0.68$, $p < 0.001$,

Table 2. Summary of Statistics of Model Performance at Each Site

	GPP_TG model		ET_This study			ET_MOD16		
Site ID	RMSE	R^2	RMSE	MRE	R^2	RMSE	MRE	R^2
US_Ha1	2.16	0.85	0.43	4.4	0.86	–	–	–
US_WCr	1.46	0.94	0.41	15.8	0.92	0.76	36.1	0.85
US_MMS	1.49	0.91	0.45	2.7	0.89	0.81	23.2	0.82
US_Bar	0.76	0.96	0.32	0.6	0.89	1.03	78.5	0.83
US_MOz	1.87	0.74	0.72	10.1	0.76	1.04	3.6	0.76
US_Me2	1.21	0.76	0.48	5.1	0.64	0.79	8.5	0.29
CA_NS1	1.17	0.85	0.22	1.1	0.95	0.51	7.1	0.70
CA_NS2	0.63	0.90	0.35	11.4	0.93	0.43	5.3	0.75
CA_NS3	1.05	0.85	0.33	4.1	0.87	0.51	20.3	0.73
CA_NS4	0.41	0.94	0.16	11.9	0.91	0.58	71.1	0.76
CA_NS5	0.75	0.92	0.24	12.2	0.92	0.65	32.8	0.71
US_Wrc	1.97	0.77	0.47	3.7	0.75	1.28	43.5	0.41
US_Syv	1.32	0.89	0.43	2.6	0.88	1.37	69.7	0.78
US_LPH	1.58	0.87	0.58	17.4	0.87	1.13	61.5	0.76
US_Ho1	1.29	0.90	0.40	18.1	0.90	–	–	–
US_NC1	1.59	0.80	0.56	14.1	0.88	–	–	–
US_Fuf	0.91	0.56	0.44	6.1	0.68	1.00	49.2	0.42
CA_NS6	1.09	0.82	0.31	8.9	0.85	0.48	17.0	0.72
CA_NS7	0.77	0.79	0.59	21.3	0.84	0.44	28.8	0.69
US_Var	1.58	0.87	0.49	38.6	0.83	–	–	–

RMSE is the root mean square error (g C/m^2/d for GPP and mm/d for ET); MRE is the mean relative error (%). Statistics of MOD16 are given in *Mu et al.* [2011]. Hyphen (–) denotes null value.

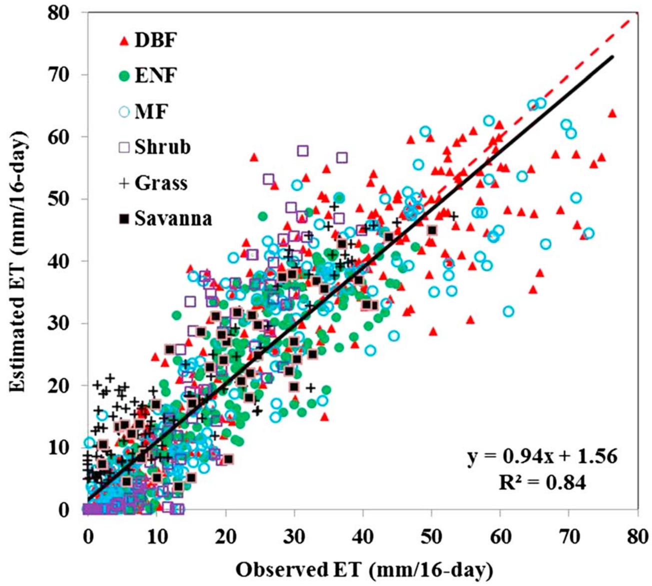

Figure 2. Comparison between observed and estimated 16 day ET at 20 Ameriflux sites. The dashed line is the 1:1 line, and the solid line indicates the best fit linear relationship.

$n = 44$), which could be ascribed to the weaker relationship between GPP and ET (Table 2 and also see auxiliary material) and lower accuracy of the TG model in estimating GPP (Table 2). Because of the strong correlation between GPP and ET, the accuracy of ET estimates depends highly on that of GPP estimates. For the remaining sites, R^2 between observed and estimated GPP by the TG model ranges from 0.74 to 0.96 and R^2 between observed and estimated ET are all larger than 0.75 ($p < 0.001$). Besides the TG model, other remote sensing-based GPP models could also be used, e.g., the chlorophyll content model [*Gitelson et al.*, 2006; *Peng et al.*, 2013]. *Wu et al.* [2011] evaluated the chlorophyll content model over 15 North American flux sites and reported that the model could provide good estimates of monthly GPP for both deciduous forest sites and nonforest sites with moderate results for evergreen forest sites.

[14] Despite the overall good performance, the proposed method tends to underestimate ET at the lower end in all sites except for the grassland site (Figure 2 and also see auxiliary material). This is mainly due to the underestimation of soil evaporation (E) during nongrowing seasons. Theoretically GPP should be a better indicator of plant transpiration (T) than total ET [*Beer et al.*, 2009]. However, T usually dominates ET, and the partitioning between E and T changes proportionally (depends mostly on surface vegetation conditions) during growing seasons, which may still result in a good GPP-ET relationship. Nevertheless, GPP and T decline toward zeros during nongrowing season, while E may still occur if temperature and water conditions permit. Although the nongrowing season is mainly defined by either low temperature or low soil moisture in natural ecosystems which implies only small E values, cautions should be paid when applying the method to cropland ecosystems where plant phenology and soil moisture conditions are profoundly impacted by human activities, e.g., irrigation.

[15] It is more encouraging to see that nearly all statistics at all sites for the proposed method show better performance than the MOD16 product (Table 2). In addition to MODIS 1 km land surface products, MOD16 uses other coarse resolution meteorological inputs and is essentially an interpolated and "pseudocontinuous" product, i.e., not truly per pixel [*Rahman et al.*, 2005]. Performance of the MODIS ET algorithm could be largely improved when in situ meteorological measurements are used [*Mu et al.*, 2011]. Another limitation in MOD16 is that the effects of soil moisture restriction on evaporation are generally reflected by meteorological forcing based on the complementary relationship, resulting in slower response of variations in energy and heat fluxes than the thermal infrared remote sensing-based ET models [*Long and Singh*, 2010]. If estimating integrated ET over longer time scales (e.g., half a month) is the main focus of studies and the MODIS ET algorithm underperforms in most cases, reliable estimates of ET based purely on satellite remote sensing demonstrated in this study should have greater robustness.

[16] In addition to the advantages in fewer inputs, the developed method circumvents up-scaling instantaneous ET estimates at satellite overpass time to daily values or longer time scales and therefore reduces possible uncertainties in extrapolating ET under clear-sky days over days without quality satellite images [*Ryu et al.*, 2012]. MODIS 16 day EVI and 8 day LST data are used in the TG model to estimate GPP and subsequently ET. These multiday composite products are more routinely available than daily MODIS data (e.g., MODIS swath LST). Effects of cloud on ET estimation have been largely reduced because the composite 8 day LST product is mainly used to capture low temperatures (e.g., nongrowing season) and drought information over a half-month period in the TG model, and these phenomena do not change substantially between clear and cloudy days. This is an advantage over those models that incorporate instantaneous remotely sensed LST.

[17] However, there are also some limitations in the study: (1) only 20 sites were used to develop the method, which may be not sufficient to come to a robust relationship to map WUE at regional scales; (2) all sites used are located on continental North America, with most regions subject to temperate or boreal climate. To make the method an option for global ET estimation, more efforts will be needed to parameterize and validate the model over different bio-climates around the world; (3) validation of the developed method was performed only at tower scales. Validation of large-scale ET estimates from this approach can also be performed using water balance closure (e.g., *Yang et al.*, 2012), and it is our ongoing work.

4. Conclusion

[18] This study developed a method to estimate terrestrial ecosystem ET from remote sensing by exploiting the linkage between water and carbon cycles. The major strength of this method is that it does not require meteorological input as used by other satellite-based ET models. This method is easy to apply, requiring only routinely available EVI and LST data at longer time scales (e.g., 16 days in MODIS products) to calculate GPP as well as the remotely sensed leaf area index and regional soil texture data set to estimate WUE. ET estimates from the proposed method compare reasonably well with flux tower measurements at all validation sites. Comparison with the MOD16 ET product shows that the

developed method generally outperforms the MOD16 algorithm. Additional efforts will be made to improve the method under lower evaporation conditions (e.g., nongrowing season).

[19] **Acknowledgments.** We are grateful to the Oak Ridge National Laboratory for providing the tower flux data from AmeriFlux Network sites; all people involved in the field work are greatly appreciated. This work is financially supported by the National Natural Science Foundation of China (Grant Nos. 51279077 and 50939004) and the National Key Technology R&D Program of China (Grant No. 2011BAD25B05).

References

Bastiaanssen, W. G. M., M. Menenti, R. A. Feddes, and A. A. M. Holtslag (1998), A remote sensing surface energy balance algorithm for land (SEBAL) - 1. Formulation, *J. Hydrol.*, *213*(1–4), 198–212.

Beer C., M. Reichstein, P. Ciais, G. D. Farquhar, and D. Papale (2007), Mean annual GPP of Europe derived from its water balance, *Geophys. Res. Lett.*, *34*, L05401, doi:10.1029/2006GL029006.

Beer C., et al. (2009), Temporal and among-site variability of inherent water use efficiency at the ecosystem level, *Glob. Biogeochem. Cycle*, *23*, GB2018, doi:10.1029/2008GB003233.

Cook, B. D., et al. (2008), Using light-use and production efficiency models to predict photosynthesis and net carbon exchange during forest canopy disturbance, *Ecosystems*, *11*, 26–44.

Desai, A. R., P. V. Bolstad, B. D. Cook, K. J. Davis, and E. V. Carey (2005), Comparing net ecosystem exchange of carbon dioxide between an old-growth and mature forest in the upper Midwest, USA, *Agric. For. Meteorol.*, *128*, 33–55.

Dore, S., T. E. Kolb, M. Montes-Helu, B. W. Sullivan, W. D. Winslow, S. C. Hart, J. P. Kaye, G. W. Koch, and B. A. Hungate (2008), Long-term impact of a stand-replacing fire on ecosystem CO_2 exchange of a ponderosa pine forest, *Glob. Change Biol.*, *14*, 1801–1820, doi:http://dx.doi.org/10.1111/j.1365-2486.2008.01613.X.

Dragoni D., H. P. Schmid, C. S. B. Grimmond, and H. W. Loescher (2007), Uncertainty of annual net ecosystem productivity estimated using eddy covariance flux measurements, *J. Geophys. Res.*, *112*, D17102, doi:10.1029/2006JD008149.

Gitelson A. A., et al. (2006), Relationship between gross primary production and chlorophyll content in crops: Implication for the synoptic monitoring of vegetation productivity, *J. Geophys. Res.*, *111*, D08S11, doi:10.1029/2005JD006017.

Goulden, M. L., et al. (2006), An Eddy Covariance Mesonet to Measure the Effect of Forest Age on Land-Atmosphere Exchange, *Glob. Change Biol.*, *12*, 2146–2162.

Gu L., T. Meyers, S. Pallard, B. Yang, M. Heuer, K. P. Hosman, Q. Liu, J. S. Riggs, D. Sluss, and S. D. Wullschleger (2007), Influences of biomass heat and biochemical energy storages on the land surface fluxes and diurnal temperature range, *J. Geophys. Res.*, *112*, D02107, doi:org/10.1029/2006JD007425.

Hadley, J. L., P. S. Kuzeja, M. J. Daley, N. G. Phillips, T. Mulcahy, and S. Singh (2008), Water use and carbon exchange of red oak- and eastern hemlock-dominated forests in the northeastern USA: Implication for ecosystem-level effects of hemlock woolly adelgid, *Tree Physiol.*, *28*, 615–627.

Haise, H. R., H. J. Haas, and L. R. Jensen (1954), Soil moisture studies of some Great Plains soil: II Field capacity as related to 1/3- atmosphere percentage, and “minimum point” related to 15- and 26- atmosphere percentages, *Soil Sci. Soc. Am. J.*, *19*(1), 20–25.

Hollinger, D. Y., et al. (2004), Spatial and temporal variability in forest–atmosphere CO2 exchange, *Glob. Change Biol.*, *10*, 1689–1706, doi:10.1111/j.1365-2486.2004.00847.X.

Irvine, J., B. E. Law, and K. A. Hibbard (2007), Post fire carbon pools and fluxes in semiarid ponderosa pine in Central Oregon, *Glob. Change Biol.*, *13*, 1748–1760, doi:10.1111/j.1365-2486.2007.01368.X.

Jenkins, J. P., A. D. Richardson, B. H. Braswell, S. V. Ollinger, D. Y. Hollinger, and M. L. Smith (2007), Refining light-use efficiency calculations for a deciduous forest canopy using simultaneous tower-based carbon flux and radiometric measurements, *Agric. For. Meteorol.*, *143*, 64–79.

Law, B. E., et al. (2002), Environmental controls over carbon dioxide and water vapor exchange of terrestrial ecosystem, *Agric. For. Meteorol.*, *113*, 97–120.

Lei, Z. D., S. X. Yang, and S. C. Xie (1988), *Soil water dynamics*, p. 407, Tsinghua University Press, Beijing.

Long, D., and V. P. Singh (2010), Integration of the GG model with SEBAL to produce time series of evapotranspiration of high spatial resolution at watershed scales, *J. Geophys. Res.*, *115*, D21128, doi:10.1029/2010JD014092.

Long, D., and V. P. Singh (2012), A Two-source Trapezoid Model for Evapotranspiration (TTME) from satellite imagery, Remote Sens, *Environ.*, *121*, 370–388.

Lu, X., and Q. Zhuang (2010), Evaluating evapotranspiration and water-use efficiency of terrestrial ecosystems in the conterminous United States using MODIS and Ameriflux data, *Remote Sens. Environ.*, *114*, 1924–1939.

Ma, S. Y., D. D. Baldocchi, L. K. Xu, and T. Hehn (2007), Inter-annual variability in carbon dioxide exchange of an oak/grass savanna and open grassland in California, *Agric. For. Meteorol.*, *147*, 157–171.

Mu, Q. Z., M. S. Zhao, and S. W. Zhang (2011), Improvements to a MODIS global terrestrial evapotranspiration algorithm, *Remote Sens. Environ.*, *115*, 1782–1800.

Noormets, A., M. J. Gavazzi, S. G. McNulty, J. Domec, G. Sun, J. S. King, and J. Chen (2010), Response of carbon fluxes to drought in a coastal plain loblolly pine forests, *Glob. Change Biol.*, *16*, 272–287, doi:10.1111/j.1365-2486.2009.01928.X.

Norman, J. M., W. P. Kustas, and K. S. Humes (1995), A two-source approach for estimating soil and vegetation energy fluxes in observations of directional radiometric surface-temperature, *Agric. For. Meteorol.*, *77*(3–4), 263–293.

Oki, T., and S. Kanae (2006), Global Hydrological Cycles and World Water Resources, *Science*, *313*(5790), 1068–1072.

Paw, U. K. T., et al. (2004), Carbon dioxide exchange between an old-growth forest and the atmosphere, *Ecosystems*, *7*, 513–524.

Peng, Y., A. A. Gitelson, and T. Sakamoto (2013), Remote sensing of gross primary productivity in crops using MODIS 250 m data, Remote Sens, *Environ.*, *128*, 186–196.

Rahman A. F., D. A. Sims, V. D. Cordova, and B. Z. El-Masri (2005), Potential of MODIS EVI and surface temperature for directly estimating per-pixel ecosystem C fluxes, *Geophys. Res. Let. 32*, L19404, doi:10.1029/2005GL024127.

Ryu, Y., et al. (2012), On the temporal upscaling of evapotranspiration from instantaneous remote sensing measurements to 8 day mean daily-sums, *Agric. For. Meteorol.*, *152*, 212–222.

Schaap, M. G., F. J. Leij, and M. T. van Genuchten (1998), Neural network analysis for hierarchical prediction of soil hydraulic properties, *Soil Sci. Soc. Am. J.*, *62*(4), 847–855.

Sims D. A., et al. (2006), On the use of MODIS EVI to assess gross primary productivity of North American ecosystems, *J. Geophys. Res.*, *111*, G04015, doi:10.1029/2006JG000162.

Sims, D. A., et al. (2008), A new model of gross primary productivity for North American ecosystems based solely on the enhanced vegetation index and land surface temperature from MODIS, *Remote Sens. Environ.*, *112*(4), 1633–1646.

Su, Z. (2002), The Surface Energy Balance System (SEBS) for estimation of turbulent heat fluxes, *Hydrol. Earth Syst. Sci.*, *6*(1), 85–99.

Urbanski S., et al. (2007), Factors controlling CO2 exchange on time scales from hourly to decadal at Harvard Forest, *J. Geophys. Res.*, *112*, G02020, doi:10.1029/2006JG000293.

Van Genuchten, M. T. (1980), A closed-form equation for predicting the hydraulic conductivity of unsaturated soils, *Soil Sci. Soc. Am. J.*, *1980*(44), 892–898.

Wu, C., J. M. Chen, and N. Huang (2011), Predicting gross primary production from the enhanced vegetation index and pootosynthetically active radiation: Evaluation and calibration, Remote Sens, *Environ.*, *115*, 3424–3435.

Yang, Y. T., and S. H. Shang (2013), A hybrid dual source scheme and trapezoid framework based evapotranspiration model (HTEM) using satellite images: algorithm and model test, *J. Geophys. Res. Atmos.*, *118*, doi:10.1002/jgrd.50259 (In Press).

Yang Y. T., S. H. Shang, and L. Jiang (2012), Remote sensing temporal and spatial patterns of evapotranspiration and the response to water management in a large irrigation district of North China.

Zhang, J., et al. (2009), Satellite-based estimation of evapotranspiration of an old-growth temperate mixed forest, *Agric. For. Meteorol.*, *149*, 976–984.